SCIENTIFIC REPORTS

OPEN

SUBJECT AREAS:
ELECTRONIC STRUCTURE
CATALYST SYNTHESIS
FUEL CELLS
ELECTROCATALYSIS

Received
15 April 2013

Accepted
7 August 2013

Published
26 August 2013

Correspondence and requests for materials should be addressed to W.X. (weilinxu@ciac.jl.cn) or W.X. (xingwei@ciac.jl.cn)

A Class of High Performance Metal-Free Oxygen Reduction Electrocatalysts based on Cheap Carbon Blacks

Xiujuan Sun[1,2,3], Ping Song[1,2], Yuwei Zhang[1,2], Changpeng Liu[1,2], Weilin Xu[1,2] & Wei Xing[1,2]

[1]State Key Laboratory of Electroanalytical Chemistry, Changchun Institute of Applied Chemistry, Chinese Academy of Science, 5625 Renmin Street, Changchun 130022, P.R. China, [2]Jilin Province Key Laboratory of Low Carbon Chemical Power, Changchun Institute of Applied Chemistry, Chinese Academy of Science, 5625 Renmin Street, Changchun 130022, P.R. China, [3]Graduate University of Chinese Academy of Science, Beijing, 100049, China.

For the goal of practical industrial development of fuel cells, cheap, sustainable and high performance electrocatalysts for oxygen reduction reactions (ORR) which rival those based on platinum (Pt) and other rare materials are highly desirable. In this work, we report a class of cheap and high-performance metal-free oxygen reduction electrocatalysts obtained by co-doping carbon blacks with nitrogen and fluorine (CB-NF).The CB-NF electrocatalysts are highly active and exhibit long-term operation stability and tolerance to poisons during oxygen reduction process in alkaline medium. The alkaline direct methanol fuel cell with the best CB-NF as cathode (3 mg/cm^2) outperforms the one with commercial platinum-based cathode (3 mg $_{Pt}$/cm^2). To the best of our knowledge, these are among the most efficient non-Pt based electrocatalysts. Since carbon blacks are 10,000 times cheaper than Pt, these CB-NF electrocatalysts possess the best price/performance ratio for ORR, and are the most promising alternatives to Pt-based ones to date.

Due to the energy crisis in the world, fuel cells are attractive as clean and sustainable energy conversion devices because they can help address the ever increasing global energy demand[1]. One of the technological bottlenecks for the industrial development of fuel cells is the development of electrocatalysts with high price/performance ratio for ORR[2,3]. To date, Pt-based materials are the most widely used electrocatalysts for ORR in fuel cells. However, Pt-based catalysts suffer from the problems, such as sluggish oxygen reduction kinetics, durability, very limited reserves, high cost, and inactivation by carbon monoxide (CO) poisoning; these obstacles hamper the commercial application of fuel cells[1]. Consequently, tremendous efforts are aimed at developing non-precious metal[2,4–8] and metal-free electrocatalysts[3,9–13] to rival Pt-based catalysts. Recently, heteroatom (N, B, S, P, Fe or Co)-doped carbon materials, such as carbon nanotubes (CNTs)[3,14,15], graphene[16–18], graphitic arrays[9] and amorphous carbon[19–22], were found to exhibit excellent electrocatalytic performance for ORR. Among these carbon-based non-Pt and metal-free catalysts, very few are on a competitive level with Pt[3–5,20]. The best of these catalysts, such as vertically aligned CNTs (VA-CNTs), CNT-graphene complexes and amorphous carbon derivatives, are as expensive or rare, if not more, than Pt. Of the carbon materials carbon blacks are the cheapest and most sustainable, and can have important implications for the commercialization of fuel cells in future[19,23].

In this study we developed a general method to obtain CB-based high performance metal-free ORR electrocatalysts by co-doping common CBs (such as BP2000 and Acetylene carbon (AC) black) with nitrogen (N) and fluorine (F). The obtained low-cost metal-free carbon catalysts showed high electrocatalytic activity of ORR in alkaline medium, which is on the same level as that of commercial Pt/C and the best non-Pt electrocatalysts ever reported[2–4]. The high performance CB-based metal-free electrocatalysts for ORR reported here possess the better price/performance ratio than any other ORR electrocatalysts reported thus far because of their extremely low cost and abundance.

Results

Synthesis of catalysts. The synthesis of CB-NF was based on a simple procedure with CB, melamine ($C_3H_6N_6$) and ammonium fluoride (NH_4F) as starting materials [see Supplementary Information (SI)]. For comparison, CB, CB-N and CB-F were also obtained in a similar way.

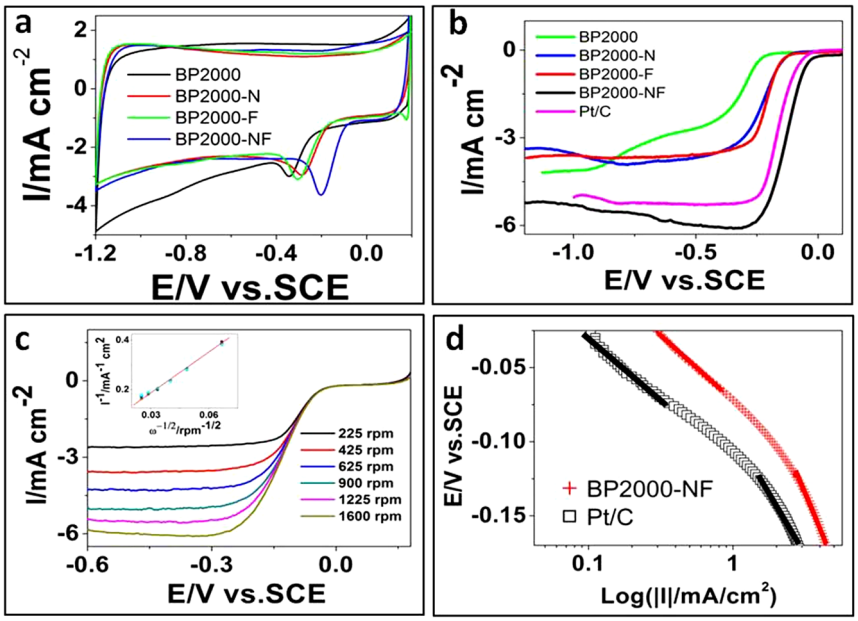

Figure 1 | Electrochemical characterization of BP2000-NF. (a) CVs of pure BP2000, BP2000-N, BP2000-F and BP2000-NF in O_2-saturated 0.1 M KOH with scan rate of 50 mV/s. (b) RDE polarization curves of pure BP2000, BP2000-N, BP2000-F, BP2000-NF and Pt/C in O_2-saturated 0.1 M KOH with scan rate of 5 mV/s and rotation speed of 1600 rpm. (c) Voltamperograms for oxygen reduction on BP2000-NF in O_2-saturated 0.1 M KOH at various rotation speeds with scan rate of 5 mV/s. Inset: K-L plots at different potentials. (d) Tafel plots for BP2000-NF and Pt/C extracted from (b). The loading of catalysts is 0.39 mg cm^{-2} for doped carbon catalysts and 24 μg_{Pt} cm^{-2} for commercial Pt/C.

Physical characterization. As an example, the BP2000-based metal-free catalysts (Supplementary Fig. S1) were introduced in detail as following. The morphology of BP2000-NF was investigated by means of scanning electron microscopy (SEM), X-ray diffraction (XRD) and Raman spectrum. As shown in Supplementary Fig. S2, the BP2000-NF particles are amorphous with an average size of ~20 nm and high content of graphitic carbon. The porous nature of BP2000-NF was assessed with nitrogen adsorption-desorption analysis (Supplementary Fig. S2). The type-IV isotherm of BP2000-NF indicated a mesoporous structure. The Brunauer-Emmett-Teller (BET) surface area of BP2000-NF with an average pore size of 11 nm was 321.8 m^2/g, much smaller than the 1391.3 m^2/g obtained for BP2000 with an average pore size of 5 nm. This difference is attributed to the collapsing of micropores to form mesopores during the annealing process.

Electrochemical characterization. To assess the catalytic activity of these catalysts for ORR, we performed cyclic voltammetry (CV) and rotating disk electrode (RDE) measurements. As Figs. 1a and 1b show, the pure BP2000 in 0.1 M KOH is sluggish for ORR, evident by the low onset potential (~−0.22 V) and the fact that it is a two-step two-electron process (Supplementary Fig. S3). Either the N- or F-doping of BP2000 can enhance the ORR activity, indicated by the higher onset potentials (~−0.15 V) and one-step four-electron process (Figs. 1a, 1b and Supplementary Fig. S3). Surprisingly, when BP2000 was co-doped by N and F, the ORR activity was greatly enhanced due to a synergetic effect between doped N and F atoms[2,14]. CV shows a peak potential at −0.20 V, which is the same as that on commercial Pt/C (E-TEK) (Fig. 1b), suggesting pronounced electrocatalytic activity of BP2000-NF. The high ORR activity of BP2000-NF is also gleaned from its much higher onset potential (~0.04 V) and half-wave potential ($E_{1/2} \approx -0.12$ V) (black in Fig. 1b), which are roughly equivalent to the performance of commercial Pt/C (pink in Fig. 1b) and the best non-Pt ORR electrocatalysts reported as well (Supplementary Fig. S4). The mass activity of BP2000-NF at $E_{1/2}$ (−0.12 V) is 6.6 A g^{-1}, making it one of the most active Pt-free ORR catalysts reported to date[3,4,20].

Typical current-potential curves of BP2000-NF in an oxygen-saturated 0.1 M KOH electrolyte are shown in Fig. 1c. The current shows a typical increase with rotation rate due to the shortened diffusion layer[20]. Analysis of the steady-state diffusion plateau currents through Kouteckey-Levich plots (inset in Fig. 1c) reveals a four-electron process (**n** = 4.2) of the ORR on BP2000-NF, with water as the main product, as is the case for Pt-based catalysts. Such high **n** value and low yield of hydrogen-peroxide (Supplementary Fig. S5) indicate good four-electron selectivity of the BP2000-NF catalyst in alkaline aqueous medium[8].

The performance of BP2000-NF was further evaluated for mechanistic and kinetic performance using Tafel plots (Fig. 1d). The Tafel slop in the low current density region on BP2000-NF is 68 mV/decade, which is very close to that on Pt/C surface. This reveals the transfer of the first electron on both of these two catalysts is the rate-determining step under Temkin conditions for the adsorption of intermediates[24]. In the high current density region, the Tafel slop is 126 mV/decade, which is the same as that on Pt/C surface. This result is attributed to a change in the mechanism of ORR from Temkin to Langmuir adsorption conditions when the current density increases[24]. From a mechanistic point of view, this would imply the ORR mechanisms on BP2000-NF and Pt-based catalysts are similar in an alkaline medium[19]. A six-times higher exchange current density (3.0×10^{-3} mA/cm^2) of BP2000-NF was obtained from Tafel plots when compared with the exchange current density (5.2×10^{-4} mA/cm^2) of commercial 20 wt% Pt/C, indicating a much higher intrinsic activity of BP2000-NF for the ORR than commercial Pt/C (E-TEK).

The tolerance of BP2000-NF to methanol or CO was also assessed with CV in an O_2 saturated electrolyte containing methanol (3 M) or CO. As shown in Fig. 2a, no activity specific to methanol or CO was observed on BP2000-NF as the characteristic peaks of ORR are maintained. These results indicate that the metal-free BP2000-NF can easily reduce O_2 but is tolerant to methanol or CO. On Pt/C (Fig. 2b) the electro-oxidation of methanol or CO seriously retards the ORR process, as indicated by the disappearance of the oxygen reduction peak. This fact indicates that the as-prepared BP2000-NF

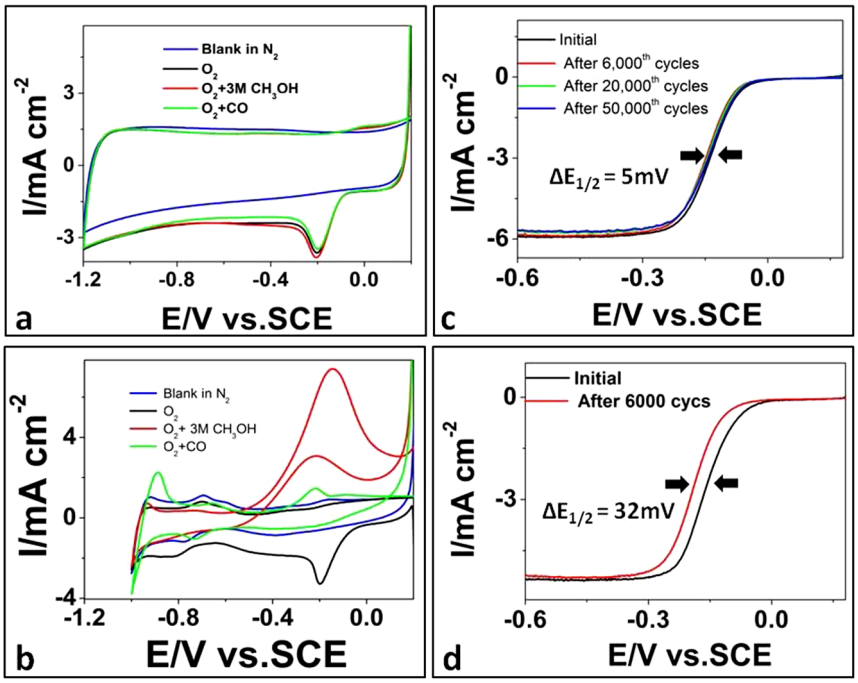

Figure 2 | The tolerance and stability of BP2000-NF and Pt/C. CVs of BP2000-NF (a) and Pt/C (b) in N_2-(blue), O_2-saturated (black), 3 M methanol O_2-saturated (red), CO- and O_2-saturated (green) 0.1 M KOH with scan rate of 50 mV/s. (c) RDE polarization curves of BP2000-NF with scan rate of 5 mV/s before and after 6000, 20,000 and 50,000 potential cycles in O_2-saturated 0.1 M KOH. (d) RDE polarization curves of Pt/C with scan rate of 5 mV/s before and after 6,000 potential cycles in O_2-saturated 0.1 M KOH.

is a nice alternative to Pt for alkaline direct methanol fuel cell as a cathode.

Based on the US Department of Energy's accelerated durability test protocol we assessed the durability or stability of the BP2000-NF catalyst by cycling the catalyst between −1.2 and 0.2 V at 200 mV s^{-1} in an O_2 saturated 0.1 M KOH[5]. As shown in Fig. 2d, a 32 mV negative shift of half-wave potential $E_{1/2}$ after 6,000 cycles shows the deterioration of Pt occurred on Pt/C. The reason could be attributed to the migration/aggregation of the Pt nanoparticls caused by continuous potential cycling and subsequent loss of the specific catalytic activity[3]. BP2000-NF showed a much smaller negative shift (5 mV) of $E_{1/2}$ (Fig. 2c) after 6,000 continuous cycles, followed by almost no change of $E_{1/2}$ after 50,000 cycles, thus exhibiting excellent long-term operation stability[4].

In order to further substantiate the higher performance of BP2000-NF over Pt/C observed above in alkaline solution; we performed alkaline direct methanol fuel cell (ADMFC) tests with BP2000-NF and commercial Pt/C as cathodes, respectively (**SI**). As shown in Fig. 3, the ADMFC with BP2000-NF as cathode catalyst (3 mg/cm^2) shows a much better performance than that with commercial Pt/C (60 wt%, 3 mg$_{Pt}$/cm^2) as cathode. Under similar conditions, the open circuit voltage of 0.8 V for the ADMFC with BP2000-NF is higher than that of 0.73 V for the cell with Pt/C, indicating a much better methanol tolerance of BP2000-NF for ORR. The maximum power density with BP2000-NF is ~15 mW/cm^2 at 60°C, compared to 13 mW/cm^2 for commercial Pt/C. The potential of the BP2000-NF cell shows almost no decrease after 24 hrs at 37°C at a fixed current of 200 mA, while the Pt/C cathode experiences a potential decrease of 10%, indicating much higher long-term operation stability for the BP2000-NF over Pt/C (Fig. 3b). All these data from ADMFCs further substantiate the high performance of BP2000-NF as an ORR catalyst in alkaline medium, and unambiguously indicate the BP2000-NF is an excellent alternative to Pt as a cathode catalyst in alkaline fuel cells, whether it be a

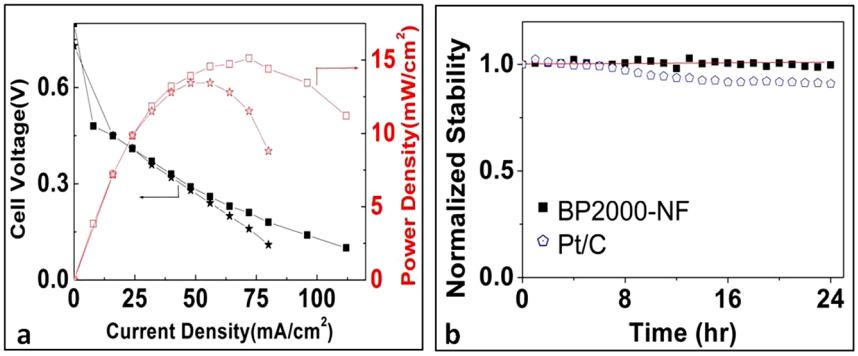

Figure 3 | The ADMFC performance with different cathodes. (a) The voltage and power density of ADMFCs at 60°C with (square) BP2000-NF (3 mg/cm^2) and (star) Pt/C (60 wt%, 3 mg $_{Pt}$/cm^2) as cathodes, respectively. (b) The normalized long-term operation stability of ADMFC potential with BP2000-NF and Pt/C as cathodes, respectively, with fixed current of 200 mA at 37°C. Anode: Pt/C (60 wt%, 3 mg $_{Pt}$/cm^2) with 2 M methanol in 2 M KOH with a flow rate of 5 mL/min, cathode: dry oxygen with flow rate of 100 mL/min.

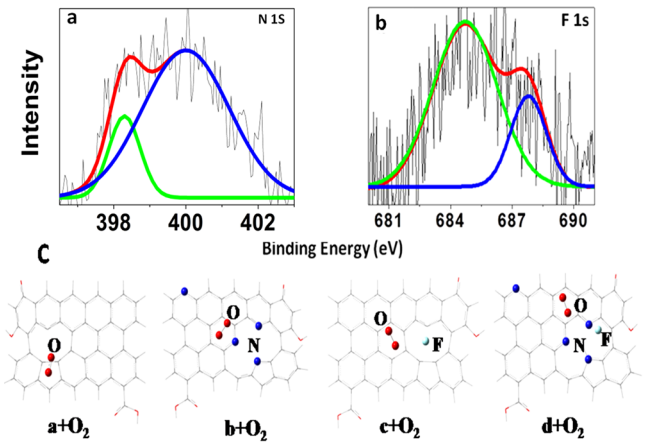

Figure 4 | High resolution N 1s (a) and F 1s (b) XPS spectra of BP2000-NF. (c) The optimized structures for models **a** + O_2, **b** + O_2, **c** + O_2 and **d** + O_2 in solution phase.

performance or cost point of view. The obtained performance of ADMFC with BP2000-NF as cathode is on par with that obtained with Pt black as cathode[25] (Supplementary Fig.S7).

Furthermore we found that our protocol can be generalized to other cheap carbon blacks to get high performance CB-NF catalysts for ORR. For example, besides BP2000-NF, the other metal-free high performance ORR catalyst (AC-NF) was also obtained by co-doping acetylene carbon (AC) with N and F atoms in the same way. It shows a similar high performance in alkaline medium (Supplementary Fig. S8).

Discussion

We proposed some reasons to elucidate a mechanism for the high activity of the BP2000-NF. Some clues can be found from the high resolution XPS spectra of N and F. As shown in Fig. 4a, BP2000-NF shows two different bonding configurations of N atoms, indicated by the peaks of N 1s at 398.3 and 399.9 eV which correspond to pyridine-like (18.9%) and pyrrole-like (81.1%) nitrogen[26]. For nitrogen-doping, certain types of N-containing functional groups, such as pyrrolyic and pyridinic groups, especially those at graphitic edge plane sites, have been claimed to be responsible for the high ORR activity, such as the high onset potential[19,27]. The high activity of BP2000-NF could then be partially attributed to the high content of pyrrole-like and pyridinic-like N. For the F-doped carbon, the following activity order has been found: ionic C-F > semi-ionic C-F > covalent C-F[28,29]. As shown in the high resolution XPS of F 1s for BP2000-NF (Fig. 4b), the contents of ionic (684.8 eV) and semi-ionic (688.0 eV) C-F bonds are 79.1% and 20.9%, respectively[28,30]. So, the high activity of BP2000-NF could also be partially attributed to the high content of ionic C-F bond which probably was formed at high temperature due to the partial break of covalent C-F bond formed at low temperature (Supplementary Fig. S6). As shown in the quantum calculation (SI), the $F^{\delta-}$ ($\delta < 1$) in the ionic or semi-ionic C-F bond is different from the free F^- physisorbed on carbon from solution[28]. In the ionic C-F bond the $F^{\delta-}$ still bonds with $C^{\delta+}$ tightly but with more ionic content compared with covalent ones. That is why the BP2000-NF is very stable even in alkaline solution observed (Fig. 2c). Furthermore, from the CVs (Fig. 1a) or polarization curves (Fig. 1b), we can see there is a synergetic effect between doped-N and -F atoms indicated by the much higher peak or plateau current, onset potential and $E_{1/2}$ on BP2000-NF compared with those on BP2000-N or BP2000-F. The higher onset potential and $E_{1/2}$ on BP2000-NF indicate each active site on it is a complex or union of doped-N, -F and carbon atoms around defects or vacancies. The new complex active site possesses much higher intrinsic activity for ORR than a single N- or F-doped active site due to a synergetic effect[2,14].

Table 1 | The optimized structures for the CB-O_2 systems and their geometry parameters in solution phase

Compound	**a** + O_2	**b** + O_2	**c** + O_2	**d** + O_2
[a]E_g(eV)	1.726	1.584	1.556	0.770
[b]$D_{O\text{-}O}$(Å)	1.217	1.241	1.254	1.258
[c]e_{O2}(e)	−0.02	−0.21	−0.31	−0.33
[d]E_{ad}(eV)	−0.04	−0.20	−0.36	−0.39

Note: [a]E_g: The energy gap between HOMO and LUMO for models **a**, **b**, **c** and **d** without O_2 adsorption.
[b]$D_{O\text{-}O}$: The bond length for O_2. [c]e_{O2}: The charge O_2 possesses.
[d]E_{ad}: The adsorption energy, and it is equal to E_{ad} = E(CB-O_2)−E(CB)−E(O_2), in which E(CB-O_2), E(CB) and E(O_2) is the total energy for CB-O_2 system, separated CB and separated O_2 molecule.

To get insight into the electrocatalytic activity of CB-NFs, four theoretical models with O_2 adsorption (**a** + O_2, **b** + O_2, **c** +O_2 and **d** + O_2 in Fig. 4c) are used to study the effect of dopants on ORR with density functional theory (DFT) method. Firstly, with the sequential doping of N and then F in parent CB (compound **a**, **b**, **c** and **d**) without O_2 adsorption, the energy gap (E_g in Table 1) between the HOMO and LUMO decreases more and more by 1.726 eV (CB), 1.584 eV (CB-N), 1.556 eV (CB-F) and then 0.770 eV (CB-NF), predicting the following order of catalytic activity due to a synergetic effect between doped N and F: CB-NF > CB-F ≥ CB-N > CB[31]. After the oxygen adsorption (Fig. 4c), the simulation showed that the bond length of adsorbed O_2 ($D_{O\text{-}O}$ in Table 1) increases to 1.241 and 1.254 Å after N- or F-doping, indicating improved activity of ORR compared with pure CB[32–34]. Interestingly, the NF-co-doping (model **d** + O_2) can further increase the bond distance of O_2 to 1.258 Å, indicating a further activation of ORR on CB-NF. In addition, it was found CB provides more electrons to adsorbed O_2 after the N or F-doping, and even more after NF-co-doping (e_{O2} in Table 1). The more electrons transferred, the easier the ORR process is[3,26,31]. The larger adsorption energy (E_{ad} in Supplementary Table 1) for O_2 on NF-co-doped CB comparing with those in the other two CB also indicates larger interaction between CB-NF and adsorbed O_2. The calculated second-order perturbation energies ($E(2)$ in Supplementary Fig. S11) show that the additional interaction between F and adjacent C-N enhances the attractive interaction between O_2 and adjacent C and N, but nearly no such interaction was found in pure CB. In other words, the synergetic effect between doped N and F can further induce larger interaction between doped CB surface and O_2, and then promote the ORR process. Moreover, there is no covalent C-F bond formation and the charge of −0.61 e in F shows the ionic character. However, the interaction between F and adjacent C (Supplementary Fig. S11) indicates incomplete ionic character for F, i.e. no free F^-, consistent with the results from XPS. These theoretical results predict the following order of catalytic activity of CB-NF > CB-F ≥ CB-N > CB, consistent with the experimental observations of exceptionally high electrocatalytic activity of BP2000-NF for ORR.

Here we have demonstrated a class of high performance metal-free ORR catalysts from cheap and sustainable carbon blacks which have been downplayed. The high performance (high activity, stability and tolerance to poisons) in alkaline medium and low cost of these CB-based metal-free ORR electrocatalysts (CB-NF) make them the highest price/performance ratio ever obtained to date for ORR electrocatalysts. The ADMFC data unambiguously substantiate BP2000-NF is the most promising alternative to Pt or other rare materials as ORR catalysts in alkaline fuel cells and open up the possibility of making a variety of other high performance carbon-based metal-free catalysts for ORR.

Methods

The synthesis of CB-NF was based on a two-step procedure with CB, melamine ($C_3H_6N_6$) and ammonium fluoride (NH_4F) as initial materials. Firstly, N-doped carbon blacks were obtained as follows: a given amount of carbon blacks and appropriate melamine were ground together in an agate ball mill for about 2 h. After that the pyrolysis of the obtained mixture was performed at 900°C for 1 h under argon atmosphere with flow rate of 80 mL/min. Secondly, the as-obtained CB-N was added into the NH_4F solution while keeping fierce stirring overnight. The final mixture was dried under vacuum at 40°C and then pyrolyzed at 400°C for 30 min, 900°C for 1 h under argon atmosphere with flow rate of 80 mL/min. For comparison, CB, CB-N or CB-F was also obtained in a similar way with or without melamine or ammonium fluoride.

1. Steele, B. C. H. & Heinzel, A. Materials for fuel-cell technologies. *Nature* **414**, 345–352 (2001).
2. Liang, Y. *et al*. Co_3O_4 nanoparticles on graphene as a synergistic catalyst for oxygen reduction reaction. *Nat Mater.* **10**, 780–786 (2011).
3. Gong, K., Du, F., Xia, Z., Durstock, M. & Dai, L. Nitrogen-doped carbon nanotube arrays with high electrocatalytic activity for oxygen reduction. *Science* **323**, 760–764 (2009).
4. Li, Y. *et al*. An oxygen reduction electrocatalyst based on carbon nanotube-graphene complexes. *Nat Nanotechnol.* **7**, 394–400 (2012).
5. Wu, G., More, K. L., Johnston, C. M. & Zelenay, P. High-performance electrocatalysts for oxygen reduction derived from polyaniline, Iron, and Cobalt. *Science* **332**, 443–447 (2011).
6. Wu, Z. *et al*. 3D Nitrogen-doped graphene aerogel-supported Fe_3O_4 nanoparticles as efficient electrocatalysts for oxygen reduction reaction. *J. Am. Chem. Soc.* **134**, 9082–9085 (2012).
7. Choi, C., Park, S. H. & Woo, L. Binary and ternary doping of nitrogen, boron, and phorphorus into carbon for enhancing electrochemical oxygen reduction activity. *ACS Nano* **6**, 7084–7091 (2012).
8. Wu, G. *et al*. Graphene-riched Co_9S_8-N-C non-precious metal catalyst for oxygen reduction in alkaline media. *ECS Trans.* **41**, 1709–1717 (2011).
9. Liang, J. L. *et al*. Facile oxygen reduction on a three-dimensionally ordered macroporous graphitic C_3N_4/Carbon composite electrocatalyst. *Angew. Chem., Int. Ed.* **51**, 3892–3896 (2012).
10. Ahmad, S. *et al*. Towards flexibility: metal free plastic cathodes for dye sensitized solar cells. *Chem. Commun.* **48**, 9714–9716 (2012).
11. Ahmad, S. *et al*. Efficient platinum-free counter electrodes for dye-sensitized solar cell applications. *Chem. Phys. Chem.* **11**, 2814–2819 (2010).
12. Ahmad, S. *et al*. Dye-sensitized solar cells based on poly (3,4-ethylenedioxythiophene) counter electrode derived from ionic liquids. *J. Mater. Chem.* **20**, 1654–1658 (2010).
13. Burschka, J. *et al*. Influence of the counter electrode on the photovoltaic performance of dye-sensitized solar cells using a disulfide/thiolate redox electrolyte. *Energy Environ. Sci.* **5**, 6089–6097 (2012).
14. Wang, S. *et al*. Vertically aligned BCN nanotubes as efficient metal-free electrocatalysts for oxygen reduction reaction: A synergetic effect by Co-doping with boron and nitrogen. *Angew. Chem., Int. Ed.* **50**, 11756–11760 (2011).
15. Yang, L. *et al*. Boron-doped carbon nanotubes as metal-free electrocatalysts for the oxygen reduction reaction. *Angew. Chem., Int. Ed.* **50**, 7132–7135 (2011).
16. Li, Y. *et al*. Nitrogen-doped graphene dots with oxygen rich functional groups. *J. Am. Chem. Soc.* **134**, 15–18 (2012).
17. Geng, D. *et al*. High oxygen-reduction activity and durability of nitrogen-doped graphene. *Energy Environ. Sci.* **4**, 760–764 (2011).
18. Yang, Z. *et al*. Sulfur-doped graphene as an efficient metal-free cathode catalyst for oxygen reduction. *ACS Nano* **6**, 205–211 (2012).
19. Xia, W., Masa, J., Bron, M., Schuhmann, W. & Muhler, M. Highly active metal-free nitrogen-containing carbon catalysts for oxygen reduction synthesized by the thermal treatment of polypyridine-carbon black mixtures. *Electrochem. Commun.* **13**, 593–596 (2011).
20. Yang, W., Fellinger, T. P. & Antonietti, M. Efficient metal-free oxygen reduction in alkaline medium on high-surface-area mesoporous nitrogen-doped carbons made from ionic liquids and nucleobases. *J. Am. Chem. Soc.* **133**, 206–209 (2011).
21. Ma, G. *et al*. Nitrogen-doped hollow carbon nanoparticles with excellent oxygen reduction performances and their electrocatalytic kinetics. *J. Phys. Chem. C* **115**, 25148–25154 (2011).
22. Chen, S. *et al*. Nitrogen-doped carbon nanocages as efficient metal-free electrocatalysts for oxygen reduction reaction. *Adv. Mater.* **24**, 5593–5597 (2012).
23. Litster, S. & McLean, G. PEM fuel cell electrodes. *J. Power Sources* **130**, 61–76 (2004).
24. Damjanovic, A. & Genshaw, M. A. Dependence of the kinetics of O_2 dissolution at Pt on the conditions for adsorption of reaction intermediates. *Electrochim. Acta* **15**, 1281–1283 (1970).
25. Lue, S. J., Pan, W., Chang, C. M. & Liu, Y. L. High-performance direct methanol alkaline fuel cells using potassium hydroxide-impregnated polyvinyl alcohol/carbon nano-tube electrolytes. *J. Power Sources* **202**, 1–10 (2012).
26. Yang, S., Feng, X., Wang, X. & Müllen, K. Graphene-based carbon nitride nanosheets as efficient metal-free electrocatalysts for oxygen reduction reactions. *Angew. Chem., Int. Ed.* **50**, 5339–5343 (2011).
27. Linfei Lai *et al*. Exploration of the active center structure of nitrogen-doped graphene-based catalysts for oxygen reduction reaction. *Energy Environ. Sci.* **5**, 7936–7942 (2012).
28. Nakajima, T., Koh, M., Gupta, V., Žemva, B. & Lutar, K. Electrochemical behavior of graphite highly fluorinated by high oxidation state complex fluorides and elemental fluorine. *Electrochim. Acta* **45**, 1655–1661 (2000).
29. Lee, W. H. *et al*. Selective-area fluorination of graphene with fluoropolymer and laser irradiation. *Nano Lett.* **12**, 2374–2378 (2012).
30. Shen, B., Chen, J., Yan, X. & Xue, Q. Synthesis of fluorine-doped multi-layered graphene sheets by arc-discharge. *RSC Advances* **2**, 6761–6764 (2012).
31. Wang, S. *et al*. BCN Graphene as efficient metal-free electrocatalysts for the oxygen reduction reaction. *Angew. Chem., Int. Ed.* **51**, 1–5 (2012).
32. Deng, D. *et al*. Iron encapsulated within pod-like carbon nanotubes for oxygen reduction reaction. *Angew. Chem., Int. Ed.* **52**, 371–375 (2012).
33. Zhang, P., Lian, J. S. & Jiang, Q. Potential dependent and structural selectivity of the oxygen reduction reaction on nitrogen-doped carbon nanotubes: a density functional theory study. *Phys. Chem. Chem. Phys.* **14**, 11715–11723 (2012).
34. Hu, X., Wu, Y., Li, H. & Zhang, Z. Adsorption and activation of O_2 on nitrogen-doped carbon nanotubes. *J. Phys. Chem. C* **114**, 9603–9607 (2010).

Acknowledgments

Work was funded by the "Hundred Talents Project" of the Chinese Academy of Sciences (110000PP65), "the Recruitment Program of Global young Experts" of China, National Natural Science Foundation of China (21273220, 21073180, and 20933004), the National Basic Research Program of China (973 Program, 2012CB932800, 2012CB215500). The computational support from Dr. Ke-Li Han is appreciated. The supply of alkaline PAEK membrane from Prof. Suo-bo Zhang is appreciated.

Author contributions

W. Xu conceived and coordinated the research. X.S. contributed to synthesis and electrochemical characterization of catalysts. P.S. contributed to the theoretical calculation. Y.Z., C.L. and W. Xing contributed to the fuel cell tests. The manuscript was primarily written by W. Xu, X.S. and P.S. All authors contributed to discussions and manuscript review.

Additional information

Supplementary information accompanies this paper at http://www.nature.com/scientificreports

Competing financial interests: The authors declare no competing financial interests.

How to cite this article: Sun, X.J. *et al*. A Class of High Performance Metal-Free Oxygen Reduction Electrocatalysts based on Cheap Carbon Blacks. *Sci. Rep.* **3**, 2505; DOI:10.1038/srep02505 (2013).